DYNAMIC BEAM SHAPING THROUGH OSCILLATED SCANNING: INSIGHTS

IOANNIS BITHARAS ET AL.*, HERIOT-WATT UNIVERSITY

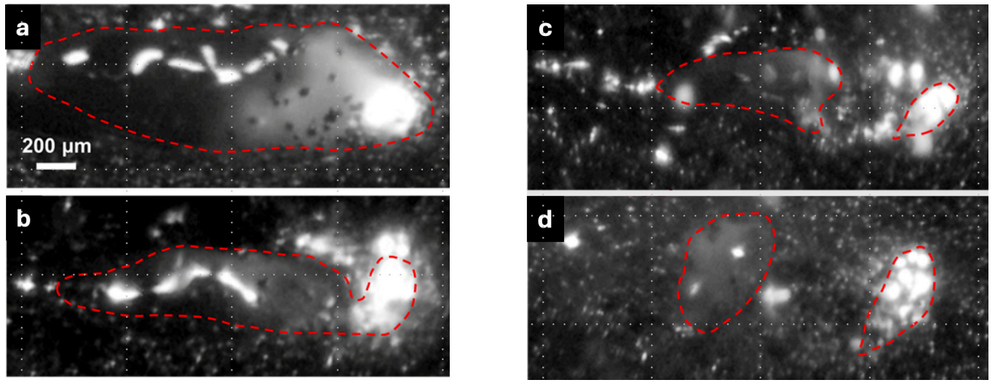

Figure 1: Observed melt pool regimes

Spatially oscillating laser powder bed fusion (SO-LPBF) is a promising scanning strategy aimed at significantly improving the performance and scalability of future metal AM machines. Unlike with conventional linear scanning, SO-LPBF employs a cycloidal laser beam trajectory, where the laser moves along continuously repeating loops, imparting heat through distinct melting and reheating phases within each cycle.

We provide the first detailed imaging and characterisation study of this scanning technique in the context of metal AM, offering deep insights into the dynamics of the melt pool, vapor jet depression, and particle ejection. We show this strategy can result in higher heat and mass accumulation towards the melt pool, enabling stable melting with the potential for processing substantially thicker powder layers.

EXPERIMENTS

To systematically explore the effects of oscillation parameters, we conducted experiments using our in-house additive manufacturing rig at Heriot-Watt University, varying the oscillation amplitude (A = 50–350 µm), frequency (f = 300–1000 Hz), and linear scan velocity (V = 25–350 mm/s). Stainless steel 316L powder layers of 125–250 µm thickness were used for line and island scans. A large volume of data was collected and multiple analyses were carried out, which can be accessed in the full research publication [1].

Two dimensionless numbers, $n = V/(f \cdot A)$ and $m = 8 \cdot V \cdot A/(f \cdot \pi \cdot D^2)$, were derived, capturing the geometric characteristics of the cycloidal scans. The amplitude-normalised pitch (n) measures loop spacing relative to oscillation amplitude, while m indicates how widely laser energy is spread relative to the beam's spot size. These dimensionless numbers allow for direct comparisons between different parameter sets and serve as predictive indicators of melt pool stability and continuity. Moreover, calculation of the average effective laser fluence (Φ_{av}), enabled rapid comparison of parameter sets.

RESULTS

Four distinct regimes emerged clearly from our analysis (Figure 1):
(a) keyhole formation at high fluence (Φ_{av} = 2.7 J/mm², m = 1, n = 0.8) due to excessive overlap of energy;
(b) optimal continuous melt pools at moderate fluence and spacing (Φ_{av} = 1.2 J/mm², m = 3.8, n = 1.9);
(c) intermittently stable melt pools at lower fluence and larger spacing (Φ_{av} = 0.7 J/mm², m = 6.8, n = 0.3), leading to inconsistent melting; and
(d) discontinuous, periodic globular deposits caused by large overlap and low average energy input (Φ_{av} = 0.4 J/ mm², m = 13.6, n = 6.7).

To evaluate SO-LPBF parameters, we used optical profilometry to measure material deposition and identify conditions producing continuous or discontinuous tracks, establishing a practical lower process limit. Figure 2 shows bead cross-sectional area versus Φ_{av} and m. Both metrics predict the transition from continuous to discontinuous tracks. Continuous tracks occurred at Φ_{av} > 1 J/mm² and m < 5.5.

We also analysed the amplitude-normalised pitch, n. Values above n > 2 consistently led to track break-up from insufficient overlap, while

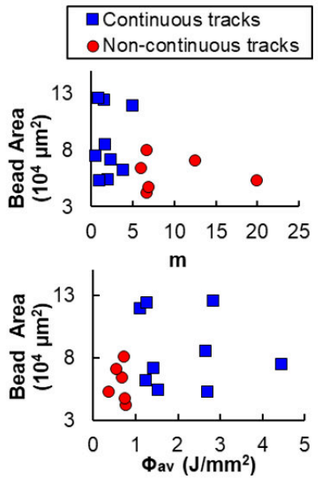

Figure 2: Bead area trends with effective fluence and energy spread metric m.

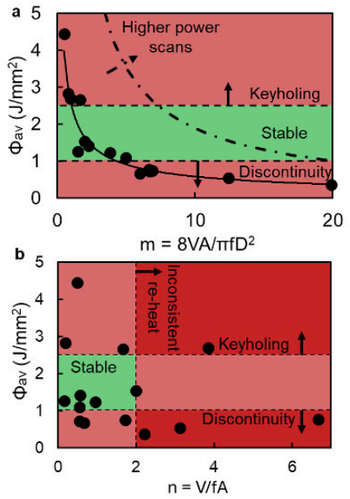

Figure 3: SO-LPBF process maps

n < 0.5 produced higher mass transfer due to longer interaction times and more effective powder entrainment. Thus, n, m, and Φ_{av} together define the lower bounds of stable processing.

ANALYSIS

To establish the upper bound, we used cross-sectional micrographs to identify the fluence threshold for keyholing and porosity. Keyhole formation was seen at Φ_{av} > 2.5 J/ mm². For example, set #A5 (Φ_{av} = 2.7 J/mm², m = 1) showed deep melt pools with spherical pores, while moderate fluence (e.g. #C, Φ_{av} = 1.2 J/mm², m = 3.8) resulted in stable pools with near-unity aspect ratios. This confirms that although wobbling improves robustness, excessive energy can still cause defects.

A semi-analytic heat conduction model, accounting for condition-dependent absorptivity, accurately predicted melt pool geometry across most stable regimes. This model constrains the SO-LPBF parameter space and provides an efficient tool for process optimisation.

Process maps constructed using the derived metrics (Figure 3) enable rapid visualisation of favourable and unfavourable operating regimes. By plotting effective fluence against the dimensionless numbers m and n, regions corresponding to continuous track formation can be distinguished from those associated with keyholing or lack of fusion. Parameter sets within 1 < Φ_{av} < 2.5 J/mm², combined with m < 5.5 and n < 2, consistently produced stable melt pools.

Complementary experiments of 5 × 5 mm² island scans with varying powder layer thickness (125 and 250 µm) confirmed that thicker layers consistently produced larger and more stable melt pools due to increased powder availability, further emphasising SO-LPBF's capability to process substantially thicker powder layers compared to conventional scanning strategies. We also observed significant powder denudation effects, with enhanced mass transfer at island edges and the first track due to greater powder availability, highlighting the influence of powder entrainment dynamics on deposited material distribution.

Microstructural analysis revealed further advantages of SO-LPBF. Without powder, the oscillation-induced melt flow consistently refined grain structures, producing fine columnar grains. When powder was introduced, grain refinement was somewhat reduced due to the modified thermal conditions, but overall grain size and form remained favourable, demonstrating SO-LPBF's potential to maintain advantageous microstructures under varied conditions.

We also introduced neuromorphic imaging for the first time in laser processing, demonstrating its potential as a powerful diagnostic tool for capturing high-speed particle dynamics. With a resolution of 8.2 µm/ pixel at 10,000 frames per second, this event-based sensor offered a unique side view of the spatter field during oscillated scanning. The neuromorphic camera recorded only changes in intensity, producing a sparse yet detailed visualisation of individual particle trajectories over time. Figure 4 shows a typical example: bright streaks represent the real-time motion of particles ejected at various angles during scanning. We observed that higher scan velocities led to reduced spatter overall, attributed to shorter interaction times between the laser and powder bed. This technology provides a new in-situ characterisation method for quantifying spatter trends across process conditions and could be valuable for feedback control in future industrial systems.

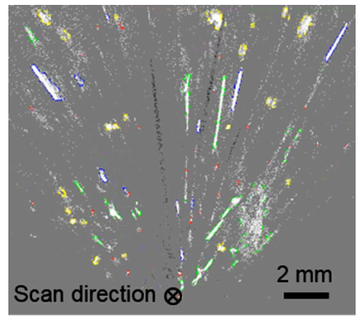

Figure 4: Event-based imaging of spatter trajectories

CONCLUSIONS

Overall, this study demonstrates that spatially oscillating LPBF is not only viable but provides a substantial step forward in productivity and process stability. Our experiments already achieved a twofold increase in productivity using current scanner technology. Importantly, the established framework, including effective fluence metrics, dimensionless parameters, and process maps, lays a solid foundation for scaling SO-LPBF to even higher laser powers and thicker powder layers. Future advances in laser sources and scanning technology could potentially unlock productivity gains by an order of magnitude, making LPBF a more competitive manufacturing option across various sectors.

REFERENCE

[1] I. Bitharas, et al. (2025) Heat and mass transfer in Spatially Oscillating LPBF. *Additive Manufacturing 109*

***I. Bitharas, K. Perkins, D. Della Crociata, G. Del Guercio, A. Clare, M. Simonelli, A.J. Moore**

I.Bitharas@hw.ac.uk
www.hw.ac.uk

Ioannis Bitharas studies laser-material interactions in manufacturing and biomedical applications, employing advanced imaging, in-situ characterisation & flow visualisation techniques.